


# Design of a Photovoltaic Simulator with a Novel Reference Signal Generator and Two-Stage LC Output Filter

Yucheng Wang \*  
Email: 1798575320@qq.com\*

**Abstract**—This paper presents a systematic design technique for a photovoltaic simulator. The proposed technique helps improve control loop bandwidth and system response. The photovoltaic equivalent circuit is used to generate the current-voltage reference curves. A novel technique is proposed and implemented with analog controllers to simplify the reference signal generator and to avoid sampling time delays in digital controllers. A two-stage LC output filter is implemented to push the resonant frequency higher and thus allowing a higher bandwidth control loop design while keeping the same switching ripple attenuation as in the conventional one-stage LC output filter. Design procedures for both control and power stage circuits are explained. Experimental results verify the steady state and transient performance of the proposed photovoltaic simulator at 2.7 kW output.

**Keywords**—Analog control, photovoltaic equivalent circuit, photovoltaic simulator, and two-stage LC filter.

## I. Introduction

Photovoltaic (PV) technologies are well known for their potential to environmental benefits, and their usage at kW-level is spreading. A photovoltaic system has several advantages such as pollution-free power generation, low maintenance cost, and extremely low operation cost [1-4]. The output voltage and current of a PV panel change non linearly according to the irradiance condition; therefore, a maximum power point tracking (MPPT) algorithm is needed for its power conditioning system [5-11]. Two methods are available for evaluating MPPT algorithm of a PV power conditioning system. The first one is to test using an actual PV panel with direct solar irradiance or an adjustable artificial light. This method is often used for low-power levels (<100 Watts) because in high-power levels there are some difficulties in power consumption, heat dissipation, and the bulky size of the testing setup. The second method is to test with a PV simulator that has a linear regulator or a switching-mode dc-dc converter along with associated controls. A high-power

PV simulator typically employs a switching-mode dc-dc converter that emulates the current and voltage output characteristic of an actual PV panel.

Design of a PV simulator can be found in many different ways. Some simulators are implemented with digital controllers that use either a lookup table in a data memory [12-14] or equations based on the semiconductor physics [15- 17] to emulate the PV output characteristic. For the first method, if several curves of measured data are stored in advance, the characteristic can match well with actual PV panel's output characteristic. However, a lot of data are needed to get a higher resolution of the PV output characteristic curves. For the second method, the PV characteristic is online processed by inserting the coefficients of the semiconductor equations. These digital controllers have a sampling delay that may limit the system bandwidth [18]. Moreover, an output LC filter with low cut-off frequency will limit the overall system bandwidth. Analog controllers are able to provide a higher bandwidth than digital ones do due to the absence of sampling delays. For this reason, PV simulators with analog controllers were proposed [19-23]. The analog controller based design employs a signal level reference generated by analog circuits and then amplifies it using a linear or switching regulator. To generate the reference signal, a photo diode with an LED [20] or a small PV cell with a light bulb [22,23] can be used. A hybrid PV simulator that has both analog and digital sections was proposed in [24].

In this paper, a PV simulator using a novel analog controller and a two-stage output LC filter is proposed. The simulator consists of a PV equivalent circuit to produce the reference current-voltage characteristic curve and a dc-dc buck converter to amplify it for high-power applications. A novel technique is proposed to emulate the PV equivalent circuit, which consists of a voltage-controlled current-source (VCCS), a voltage-controlled voltage-source (VCVS), a series connected diode stack or an actual PV cell, and a resistors net-

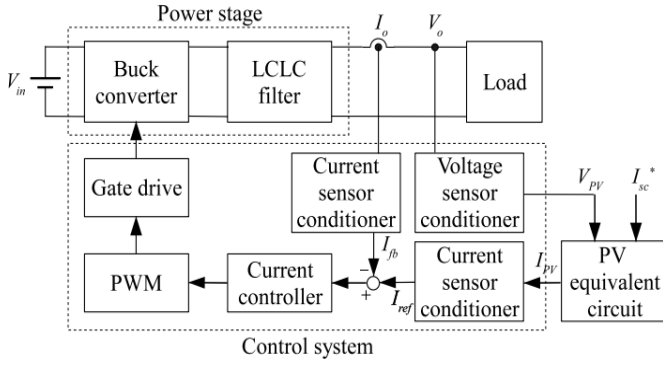


Figure 1: The entire system block diagram

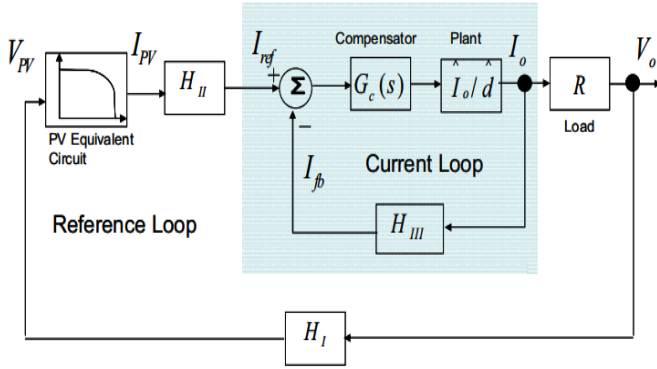


Figure 2: Control system block diagram

work. This equivalent circuit is closed-loop controlled and can generate a reference with higher than 20-kHz bandwidth. The dc-dc buck converter takes the reference signal and amplifies it with pulse-width-modulation (PWM) to produce high voltage and high current at the output, which is then filtered by the proposed two-stage LC filter. As two-stage LC filter's resonant frequency is high, the control-loop bandwidth can be improved while maintaining the same switching ripple attenuation as compared to that of the one-stage LC filter. This paper describes the design procedure in detail. Measured frequency domain response of the PV equivalent circuit, hardware setup, and experimental results will be shown to verify the design concept.

## II. SYSTEM DESCRIPTION AND CONTROL STRATEGY

The entire system block diagram is shown in Fig. 1. There are three major circuit sections: (1) PV equivalent circuit, (2) control system circuit, and (3) power stage circuit. The PV equivalent circuit consisting of a VCCS loop and a VCVS loop produces the current-voltage reference curve and feeds it to the power stage circuit through the control system circuit. The power stage circuit is a buck converter switching stage along

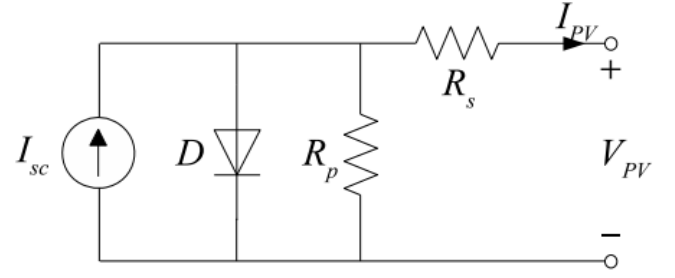


Figure 3: A PV equivalent circuit

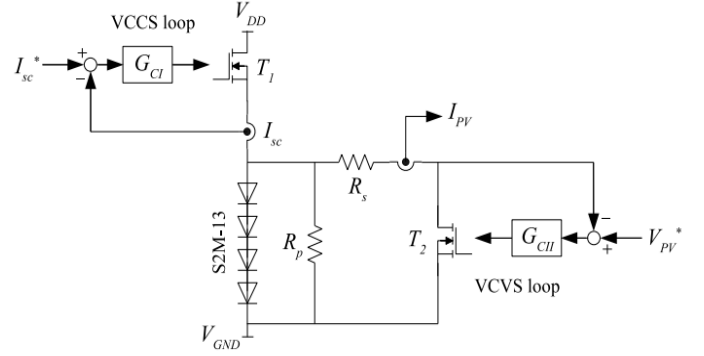


Figure 4: Experimental PV equivalent circuit with diodes

with a two-stage LC filter. Fig. 2 shows the control system block diagram. There are two control loops: (1) inner-current loop and (2) outer-reference loop. The inner-current loop controls the output current  $I_o$  of the power stage. The outer-reference loop senses the output voltage  $V_o$  of the power stage and feeds it back to the PV equivalent circuit. This circuit generates a reference current  $I_{PV}$  that will force the power stage to produce an actual PV current-voltage curve. For stability consideration, the inner-current loop should be faster than the outer-reference loop. Conditioning circuit gains  $H_I$ ,  $H_{II}$ , and  $H_{III}$  determine the voltage and current values of the power stage. Resistor  $R$  represents the equivalent load resistance of the PV power conditioning system. The detailed design procedure for both loops will be discussed in the next section.

## III. DESIGN PROCEDURE AND SYSTEM CONFIGURATION

### A. PV Equivalent Circuit Design with Diodes

A PV equivalent circuit is shown in Fig. 3 [25]. Current source  $I_{sc}$  is proportional to the solar irradiance ( $W/m^2$ ), and diode  $D$  is a typical pn junction diode. Resistor  $R_p$  represents the leakage current along the cell borders and localized short circuits while resistor  $R_s$  represents the resistive paths through the semicon-

ductor material and contacts [26]. The current-voltage characteristic of this circuit can be designed to match with the actual PV cell or PV panel.

Fig. 4 illustrates the experimental version of the PV equivalent circuit. The circuit shown in Fig. 3 is built with analog components to generate the current-voltage output reference curves. Current source  $I_{sc}$  is represented by a voltage-controlled current-source (VCCS) loop. MOSFET T1 operates in the linear region so current  $I_{sc}$  will be controlled to follow the current reference  $I_{sc}^*$ . In the voltage-controlled voltage-source (VCVS) loop, MOSFET T2 operates in the linear region to control the output terminal voltage of the PV equivalent circuit VPV. With the use of VCCS, there is no need to use an external light source. As for the diode D, its I-V characteristic affects the generated PV reference curve. Therefore, it should be selected to match with actual PV characteristic. In this design, four series-connected diodes (model number: S2M-13) were used in the experimental PV equivalent circuit. A high bandwidth for both the VCCS loop and the VCVS loop should allow decoupling between the reference signal and the outer loop dynamics. Fig. 5 shows the measured compensated loop gain for both the VCCS loop and the VCVS loop, respectively. The VCCS loop was designed to have a cross-over frequency of 90-kHz and 60° phase margin, and the VCVS loop was designed to have 20-kHz cross-over frequency with 50° phase margin. Since the performance of the VCCS loop affects the desired magnitude and response of IPV, its bandwidth should be faster than that of the VCVS loop.

The VCCS loop controller GCI(s) consists of an integrator and a set of double poles and double zeros, which is known as “type 3” controller [27]. The VCVS loop controller GCII(s) consists of an integrator and a set of pole and zero, which is known as “type 2” controller. Using the controller circuit parameters obtained from the above design, a hardware circuit that emulates PV characteristic is built and tested. Fig. 6 shows the experimental results of the current-voltage reference curves using the PV equivalent circuit shown in Fig. 4.

#### B. PV Equivalent Circuit Design with Actual PV Cell

Another approach to emulate the PV characteristic is to use an actual PV cell as a reference signal generator. Fig. 7 represents the PV equivalent circuit of this approach. This circuit is obtained by the equivalent transformation of the circuit in Fig. 3 using Thévenin’s theorem. The left part of the circuit consists of a diode D and resistors  $R_p$  and  $R_s$ . This part is equivalent to the PV equivalent circuit with  $I_{sc} = 0$ . Therefore, this part can be implemented with the actual PV cell under no illumination or in total darkness, while the current

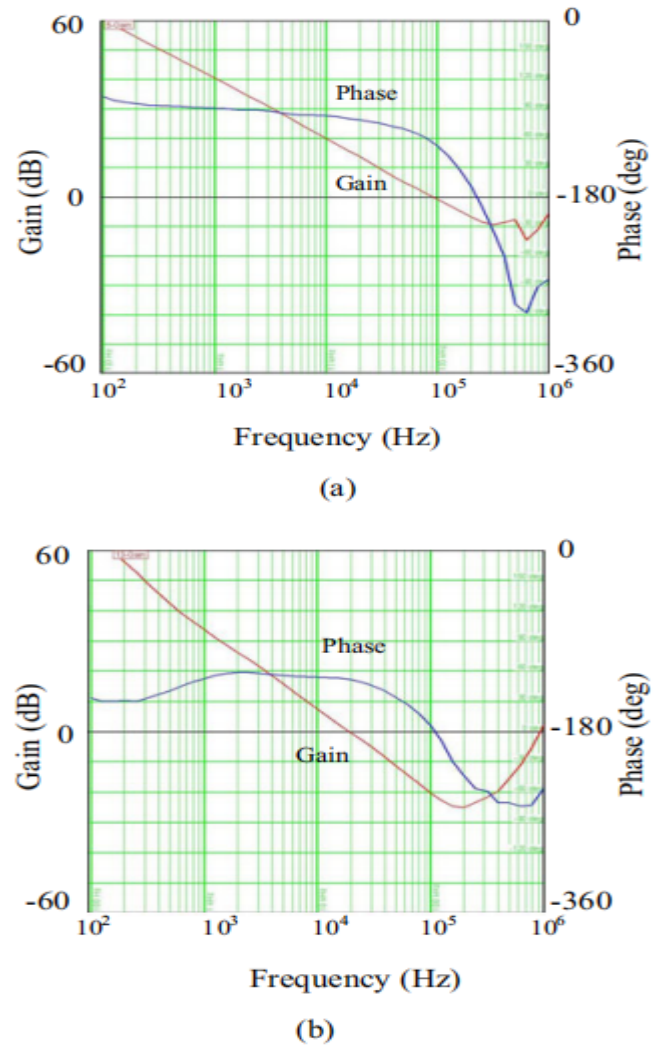


Figure 5: Measured compensated loop gain; (a) Voltage-controlled current-source loop and (b) Voltage-controlled voltage-source loop

source  $I_{sc}$  is produced with an external VCCS circuit. In this case, there is no need for any external light source, similar to the previous case using series diodes to emulate the PV cell characteristic. Fig. 8 illustrates the experimental version of this PV equivalent circuit with the use of a small un-illuminated PV cell. The circuit is built with analog

## IV. EXPERIMENTAL RESULTS

The proposed PV simulator has been built, and its photograph is shown in Fig. 13. A resistor bank was used as the load. The voltage sensor gain HI and the current sensor gains HII and HIII are set to be 0.014, 4, and 0.2, respectively. Therefore, the open-circuit voltage and short-circuit current will be 250 V (= 3.5 V / 0.014) and 20 A (= 1.0 A \* 4 / 0.2).

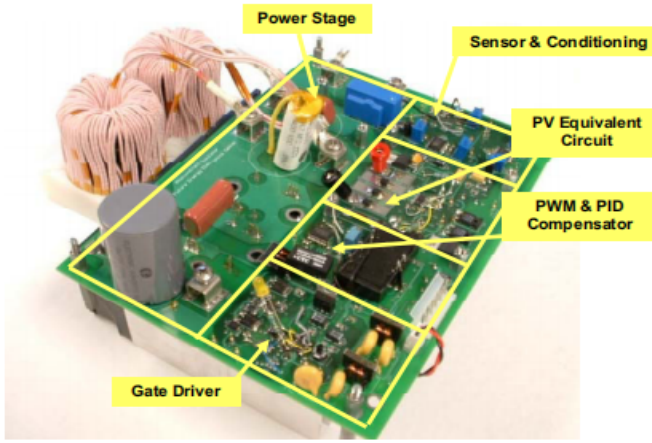


Figure 6: Photograph of the proposed PV simulator

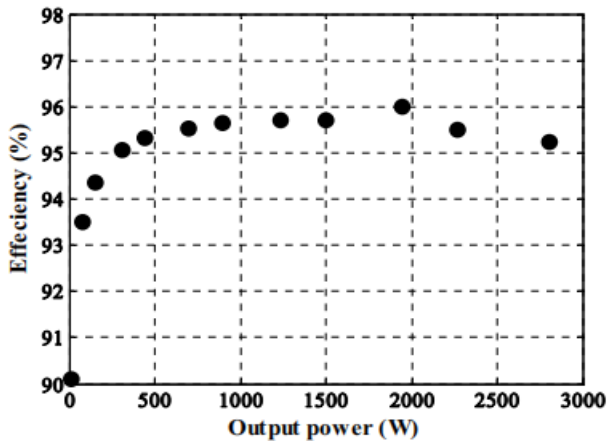


Figure 7: Photovoltaic simulator efficiency measurement curve

The overall power conversion gain is about 1400. The maximum output power was tested up to 2.7 kW. With higher input voltage and sufficient cooling of the power stage, this power level can be further increased. Fig. 14 shows the measured efficiency results of the photovoltaic simulator at different output power levels. The efficiency maintains in between 95 to 2.7-kW power output.

#### A. With PV Equivalent Circuit Using Diodes

This section shows test results using the PV equivalent circuit with series-connected diodes shown in Fig. 4 to generate the reference current signal  $I_{PV}$ . The PV curves shown in Fig. 15 were generated by the power stage at different irradiance reference levels. The results match with the current-voltage reference curve in Fig. 6 with the desired conversion ratios. Fig. 16 illustrates the output voltage  $v_o$  and current  $i_o$  waveforms for a step load change (76 to 9). Response time was recorded to be 3.8 ms.

Fig. 17 shows the output voltage  $v_o$  and current  $i_o$  waveforms of the PV simulator under different irradiance levels and perturbing frequencies. The current source  $I_{sc} *$  corresponds to irradiance level, which is a triangular wave and serves as the reference. The output voltage and current of the power stage  $v_o$  and  $i_o$  should follow the given reference. Fig. 17(a) shows the results of slow perturbation using a 10-Hz triangular wave as the reference. The output voltage and current follow the reference very well. Fig. 17(b) shows the results of fast perturbation using a 40-Hz triangular wave as the reference. In this case, the output voltage and current can not exactly follow the reference, resulting in waveform distortion. Since the time interval of most MPPT control algorithm is more than one second, and a fast perturbation with higher than 10-Hz frequency rarely occur. Therefore, the response of this photovoltaic simulator is sufficient for evaluating the MPPT control algorithms of the PV power conditioning systems.

#### B. With PV Equivalent Circuit Using an Actual PV Cell

This section shows the test results using a polycrystalline PV cell based simulator shown in Fig. 8. Fig. 18 shows the current-voltage curve generated by the power stage with  $I_{sc} * = 0.4$ -A and offset voltage  $R_{slsc} = 1.0$ -V. The result matches the basic cell characteristic shown in Fig. 9 with a desired voltage and current conversion ratios. The perturbation test results are not shown because they are the same as those shown in Fig. 17.

## V. CONCLUSION

A systematic design approach is proposed and described in detail for a PV simulator, which consists of a PV equivalent circuit and power stage circuit. The PV equivalent circuit is implemented with a novel analog circuit using high bandwidth voltage-controlled current-source and voltage-controlled voltage-source to generate high precision current-voltage reference curves in order to eliminate the sampling time delay in digital controllers. The power stage consists of a buck converter and a two-stage LC output filter with a high cut-off frequency to allow a high control loop bandwidth while keeping the same switching ripple attenuation as a one-stage LC output filter does.

The proposed PV simulator hardware prototype has been designed and built. Two approaches of generating the current-voltage reference signal using a series diode stack and an actual PV cell were implemented. Both approaches show power stage output matches the actual PV characteristic with the desired conversion ratios. Experimental results showed high accuracy and



reasonably fast response. Power level of 2.7 kW has been demonstrated. In summary, the proposed PV simulator has the following features:

## REFERENCES

### References

- [1] J. V. L. Pedrosa, K. M. Silva, and T. R. Honorato, "Experimental evaluation of an alternative generalized alpha plane applied to busbar differential protection," in *2019 Workshop on Communication Networks and Power Systems (WCNPS)*, 2019, pp. 1–5.
- [2] D. G. V. Gonçalves, F. L. de Caldas Filho, L. M. C. E. Martins, G. de O. Kfour, B. V. Dutra, R. de O. Albuquerque, and R. T. de Sousa, "Ips architecture for iot networks overlapped in sdn," in *2019 Workshop on Communication Networks and Power Systems (WCNPS)*, 2019, pp. 1–6.
- [3] J. C. L. Pereira, Y. Poledna, E. P. Ribeiro, J. S. Dias, G. Oliveira, R. Kuiava, G. V. Leandro, J. A. Vilela, R. Demonti, and A. Pedretti, "Monitoring micro phasor measurement units at university campus," in *2019 Workshop on Communication Networks and Power Systems (WCNPS)*, 2019, pp. 1–4.
- [4] M. Cristalino C. de Almeida and F. V. Lopes, "Evaluation of transmission line phase comparison protection considering the use of mimic filter," in *2019 Workshop on Communication Networks and Power Systems (WCNPS)*, 2019, pp. 1–4.
- [5] R. T. Toledo, K. M. e Silva, and T. da Rocha Honorato, "Evaluating single-phase reclosing on distribution grid voltage," in *2019 Workshop on Communication Networks and Power Systems (WCNPS)*, 2019, pp. 1–5.
- [6] D. A. do Nascimento, S. S. Refaat, A. Darwish, Q. Khan, H. Abu-Rub, and Y. Iano, "Investigation of void size and location on partial discharge activity in high voltage xlpe cable insulation," in *2019 Workshop on Communication Networks and Power Systems (WCNPS)*, 2019, pp. 1–6.
- [7] G. A. da Cunha, F. V. Lopes, and T. da Rocha Honorato, "Influence of traveling wave detection sensitivity on transient pattern recognition-based single-ended fault location approach," in *2019 Workshop on Communication Networks and Power Systems (WCNPS)*, 2019, pp. 1–5.
- [8] F. L. L. de Mendonça, D. F. da Cunha, B. J. G. Praciano, M. da Rosa Zanatta, J. P. C. L. da Costa, and R. T. de Sousa, "P2piot: A peer-to-peer communication model for the internet of things," in *2019 Workshop on Communication Networks and Power Systems (WCNPS)*, 2019, pp. 1–5.
- [9] J. S. Costa, R. T. Toledo, L. A. Gama, G. B. Santos, F. V. Lopes, P. S. Pereira, G. S. Salge, and M. J. B. B. Davi, "Investigation on full-converter-based wind power plant behavior during short-circuits," in *2019 Workshop on Communication Networks and Power Systems (WCNPS)*, 2019, pp. 1–4.
- [10] M. S. Monteiro, F. L. de Caldas Filho, L. A. Barbosa, L. M. C. E. Martins, J. T. M. de Menezes, and D. A. da Silva Filho, "University campus microclimate monitoring using iot," in *2019 Workshop on Communication Networks and Power Systems (WCNPS)*, 2019, pp. 1–5.
- [11] Y. Poledna, J. L. Pereira, and E. P. Ribeiro, "Network traffic analysis of micro pmu communication at university campus," in *2019 Workshop on Communication Networks and Power Systems (WCNPS)*, 2019, pp. 1–4.
- [12] G. P. da Silva Junior and L. S. Barros, "Synchronverter operation in active and reactive support mode," in *2019 Workshop on Communication Networks and Power Systems (WCNPS)*, 2019, pp. 1–5.
- [13] F. L. de Caldas Filho, R. L. Rocha, C. J. B. Abbas, L. M. C. E. Martins, E. D. Canedo, and R. T. de Sousa, "Qos scheduling algorithm for a fog iot gateway," in *2019 Workshop on Communication Networks and Power Systems (WCNPS)*, 2019, pp. 1–6.
- [14] T. da Silva, A. Costa, D. da Silva, L. Castro, J. Araujo, and G. Cavalcante, "Radio propagation for the amazon region considering the river level," in *2019 Workshop on Communication Networks and Power Systems (WCNPS)*, 2019, pp. 1–4.
- [15] E. S. C. Vilaça, T. P. B. Vieira, R. T. de Sousa, and J. P. C. L. da Costa, "Botnet traffic detection using rpca and mahalanobis distance," in *2019 Workshop on Communication Networks and Power Systems (WCNPS)*, 2019, pp. 1–6.
- [16] M. C. Oliveira and R. A. Ramos, "Design and simulation of a controller for emulation of a wind turbine by a dc motor," in *2019 Workshop on Communication Networks and Power Systems (WCNPS)*, 2019, pp. 1–5.
- [17] M. F. K. B. Couras, P. H. de Pinho, G. Favier, J. P. C. L. da Costa, V. Zarzoso, and A. L. F. de Almeida, "Multidimensional cx decomposition of tensors," in *2019 Workshop on Communication Networks and Power Systems (WCNPS)*, 2019, pp. 1–4.
- [18] T. André Pereira De Oliveira, A. de Leles Ferreira Filho, and E. Geraldo Domingues, "Technical analysis of a real and optimized concentrated solar power plant in the brazilian scenario," in *2019 Workshop on Communication Networks and Power Systems (WCNPS)*, 2019, pp. 1–5.
- [19] T. Spadini, G. S. Imai Aldeia, G. Barreto, K. Alves, H. Ferreira, R. Suyama, and K. Nose-Filho, "On the application of segan for the attenuation of the ego-noise in the speech sound source localization problem," in *2019 Workshop on Communication Networks and Power Systems (WCNPS)*, 2019, pp. 1–4.
- [20] A. T. Vasques and J. J. C. Gondim, "Amplified reflection ddos attacks over iot mirrors: A saturation analysis," in *2019 Workshop on Communication Networks and Power Systems (WCNPS)*, 2019, pp. 1–6.
- [21] M. E. C. Bento and R. A. Ramos, "A new pmu placement method for the assessment of the voltage stability margin," in *2019 Workshop on Communication Networks and Power Systems (WCNPS)*, 2019, pp. 1–5.
- [22] L. G. P. Vicente and M. Sharma, "Constellation design for digital communications using vector quantization," in *2019 Workshop on Communication Networks and Power Systems (WCNPS)*, 2019, pp. 1–4.
- [23] A. A. Y. R. Fares, F. L. de Caldas Filho, W. F. Giozza, E. D. Canedo, F. L. Lopes de Mendonça, and G. D. Amvame Nze, "Dos attack prevention on ips sdn networks," in *2019 Workshop on Communication Networks and Power Systems (WCNPS)*, 2019, pp. 1–7.
- [24] A. C. Salles Ramos and F. D. Freitas, "Multibus system unconstrained economic dispatch problem solution via holomorphic embedding method," in *2019 Workshop on Communication Networks and Power Systems (WCNPS)*, 2019, pp. 1–6.
- [25] I. V. Brandão, J. P. C. L. da Costa, G. A. Santos, B. J. G. Praciano, F. C. M. D. Júnior, and R. T. de S. Júnior, "Classification and predictive analysis of educational data to improve the quality of distance learning courses," in *2019 Workshop on Communication Networks and Power Systems (WCNPS)*, 2019, pp. 1–6.
- [26] L. C. de Almeida, R. T. de Sousa, A. S. Nery, D. A. da Silva Filho, E. D. Canedo, and R. R. Nunes, "Design and evaluation of an snmp-based energy consumption monitoring system for electrical grids," in *2019 Workshop on Communication Networks and Power Systems (WCNPS)*, 2019, pp. 1–6.
- [27] A. Marcondes, H. F. Scherer, J. R. C. Salgado, and R. L. B. de Freitas, "Sodium-nickel chloride single cell battery electrical model – discharge voltage behavior," in *2019 Workshop on Communication Networks and Power Systems (WCNPS)*, 2019, pp. 1–4.
- [28] J. F. Figueiredo and V. L. do Nascimento, "Broadband microstrip antenna array with circular polarization on ku band," in *2019 Workshop on Communication Networks and Power Systems (WCNPS)*, 2019, pp. 1–5.
- [29] Y. I. Ribeiro Damasceno, R. L. de Araújo Ribeiro, T. de Oliveira Alves Rocha, and S. de Cavalcante Paiva, "A control strategy with seamless mode transition for a low-voltage distributed generation system without an energy storage system," in *2018*

*Workshop on Communication Networks and Power Systems (WCNPS)*, 2018, pp. 1–6.

- [30] E. G. Sousa and S. R. M. J. Rondineau, "Computational design of a ferrite-less pi topology circulator," in *2018 Workshop on Communication Networks and Power Systems (WCNPS)*, 2018, pp. 1–5.
- [31] T. L. von Sperling, B. de A. França, F. L. de Caldas Filho, L. M. C. e Martins, R. de O. Albuquerque, and R. T. de Sousa, "Evaluation of an iot device designed for transparent traffic analysis," in *2018 Workshop on Communication Networks and Power Systems (WCNPS)*, 2018, pp. 1–5.
- [32] T. R. Honorato and K. M. Silva, "Half-cycle dft-based phasor estimation algorithm for numerical digital relaying," in *2018 Workshop on Communication Networks and Power Systems (WCNPS)*, 2018, pp. 1–4.
- [33] M. S. R. Leal, L. D. Simões, R. L. S. França, M. M. Leal, F. B. Costa, and F. E. Taveiros, "Methodology to perform real-time simulation of power systems using a fpga-based platform," in *2018 Workshop on Communication Networks and Power Systems (WCNPS)*, 2018, pp. 1–5.
- [34] G. E. Mendoza, V. M. Vacas, and N. R. Ferreira, "Optimal capacitor allocation and sizing in distribution networks using particle swarm optimization algorithm," in *2018 Workshop on Communication Networks and Power Systems (WCNPS)*, 2018, pp. 1–5.
- [35] F. E. V. Taveiros, M. R. Marques, L. S. Barros, and F. B. Costa, "Performance of the doubly-fed induction generator during a voltage sag," in *2018 Workshop on Communication Networks and Power Systems (WCNPS)*, 2018, pp. 1–5.
- [36] S. d. Cavalcante Paiva, D. Keuton Alves, F. B. Costa, R. Lúcio de Araújo Ribeiro, and T. O. Alves Rocha, "Real-time impedance estimation in grid-connected photovoltaic system using the discrete fourier transform," in *2018 Workshop on Communication Networks and Power Systems (WCNPS)*, 2018, pp. 1–5.
- [37] B. S. Soares Pereira and T. Luis Maia Santos, "Speed and reactive power regulation of doubly-fed induction generator using model predictive control," in *2018 Workshop on Communication Networks and Power Systems (WCNPS)*, 2018, pp. 1–4.
- [38] A. G. Martins-Britto, S. R. M. J. Rondineau, and F. V. Lopes, "Transient response of the grounding grid of a power line tower subject to a lightning discharge," in *2018 Workshop on Communication Networks and Power Systems (WCNPS)*, 2018, pp. 1–5.
- [39] C. M. S. Ribeiro and F. V. Lopes, "Traveling wave-based differential protection applied to hybrid transmission lines with multiple sections," in *2018 Workshop on Communication Networks and Power Systems (WCNPS)*, 2018, pp. 1–5.
- [40] D. A. Ando, R. K. Miranda, J. P. C. L. da Costa, and M. T. de Oliveira, "A novel direction of arrival estimation algorithm via received signal strength of directional antennas," in *2018 Workshop on Communication Networks and Power Systems (WCNPS)*, 2018, pp. 1–5.
- [41] P. C. Fernandes, H. Naomira Gomes Venzi Gonçalves, K. Melo e Silva, and F. Vigolvino Lopes, "Two-terminal modal traveling wave-based fault location method for hvdc systems," in *2018 Workshop on Communication Networks and Power Systems (WCNPS)*, 2018, pp. 1–4.
- [42] A. C. Santos Junior, F. D. Freitas, and L. F. J. Fernandes, "An efficient starting point to adaptive holomorphic embedding power flow methods," in *2018 Workshop on Communication Networks and Power Systems (WCNPS)*, 2018, pp. 1–5.
- [43] R. M. Gonzaga, J. A. D. Massignan, C. D. Maciel, J. B. A. London, R. M. A. de Almeida, and M. H. M. Camillo, "An embedded state estimator for reducing data volume and processing in smart grids monitoring," in *2018 Workshop on Communication Networks and Power Systems (WCNPS)*, 2018, pp. 1–5.
- [44] L. G. Cordero Bautista and P. Bueno de Araujo, "Analysis of the influence of ipfc-pod and pss controllers coordinated tuning by an adaptive genetic algorithm with hyper-mutation," in *2018 Workshop on Communication Networks and Power Systems (WCNPS)*, 2018, pp. 1–5.
- [45] M. E. C. Bento and R. A. Ramos, "Analysis of the load growth direction variation in the dynamic security assessment," in *2018 Workshop on Communication Networks and Power Systems (WCNPS)*, 2018, pp. 1–5.
- [46] J. P. A. Maranhão and J. Paulo C. L. da Costa, "Antenna array based framework for detection and localization of correlated signals," in *2018 Workshop on Communication Networks and Power Systems (WCNPS)*, 2018, pp. 1–5.
- [47] M. R. Marques, M. M. Leal, F. B. Costa, and L. S. Barros, "Assessment of wavelet-based directional overcurrent protection in a distribution system with dfig," in *2018 Workshop on Communication Networks and Power Systems (WCNPS)*, 2018, pp. 1–5.
- [48] E. P. A. Ribeiro, F. V. Lopes, J. P. G. Ribeiro, and E. J. S. Leite, "Atp/models differentiator-smoother filter model validated using actual time-domain relay," in *2018 Workshop on Communication Networks and Power Systems (WCNPS)*, 2018, pp. 1–4.
- [49] "Wcnps 2018 preface," in *2018 Workshop on Communication Networks and Power Systems (WCNPS)*, 2018, pp. i–i.
- [50] "Wcnps 2018 reviewers," in *2018 Workshop on Communication Networks and Power Systems (WCNPS)*, 2018, pp. i–i.
- [51] R. G. Baily and K. M. Silva, "Busbar differential protection based on generalized alpha plane," in *2017 Workshop on Communication Networks and Power Systems (WCNPS)*, 2017, pp. 1–4.
- [52] L. M. Peres and K. M. Silva, "Parametric sensitivity analysis of power transformer differential protection," in *2017 Workshop on Communication Networks and Power Systems (WCNPS)*, 2017, pp. 1–3.
- [53] A. C. Santos, F. D. Freitas, and L. F. J. Fernandes, "Holomorphic embedding approach as an alternative method for solving the power flow problem," in *2017 Workshop on Communication Networks and Power Systems (WCNPS)*, 2017, pp. 1–4.
- [54] A. P. Escudero, F. A. Moreno Vasquez, K. Melo e Silva, and F. V. Lopes, "Low-impedance busbar differential protection modeling and simulation using atp/emtp," in *2017 Workshop on Communication Networks and Power Systems (WCNPS)*, 2017, pp. 1–4.
- [55] A. C. Pereira Silva and L. R. A. X. de Menezes, "Estimating the error between analytical and numerical finite difference solutions of laplace equation," in *2017 Workshop on Communication Networks and Power Systems (WCNPS)*, 2017, pp. 1–4.
- [56] S. Gorlow, J. P. C. L. da Costa, and M. Haardt, "A root-cma algorithm for multi-user separation," in *2017 Workshop on Communication Networks and Power Systems (WCNPS)*, 2017, pp. 1–5.
- [57] M. da Rosa Zanatta, R. K. Miranda, J. P. C. L. da Costa, F. Antreich, and D. V. Lima, "Antenna array based receivers for third generation global positioning system," in *2017 Workshop on Communication Networks and Power Systems (WCNPS)*, 2017, pp. 1–4.
- [58] T. L. von Sperling, F. L. de Caldas Filho, R. T. de Sousa, L. M. C. e Martins, and R. L. Rocha, "Tracking intruders in iot networks by means of dns traffic analysis," in *2017 Workshop on Communication Networks and Power Systems (WCNPS)*, 2017, pp. 1–4.
- [59] E. J. S. Leite and F. V. Lopes, "Traveling wave-based fault location formulation for hybrid lines with two sections," in *2017 Workshop on Communication Networks and Power Systems (WCNPS)*, 2017, pp. 1–4.
- [60] F. M. de Magalhães, B. C. Ribeiro Monteiro, and F. V. Lopes, "Using current traveling waves to implement directional elements in parallel lines," in *2017 Workshop on Communication Networks and Power Systems (WCNPS)*, 2017, pp. 1–5.
- [61] Y. G. I. Acle and F. D. Freitas, "Shift parameter sensitivity on the computation of unstable reduced order model via truncated balanced method," in *2017 Workshop on Communication Networks and Power Systems (WCNPS)*, 2017, pp. 1–4.

- [62] J. R. Gama and F. V. Lopes, "On compensating synchronization errors in two-terminal based fault location approaches," in *2017 Workshop on Communication Networks and Power Systems (WCNPS)*, 2017, pp. 1–4.
- [63] E. A. Custódio, F. V. Lopes, and J. P. G. Ribeiro, "Ccvrt impact on the td21 function security," in *2017 Workshop on Communication Networks and Power Systems (WCNPS)*, 2017, pp. 1–4.